



## Full Length Article

## Practice and validation of inversion of seismic source localisation based on genetic algorithm

Quan Zhang, Junpeng Zou\*, Yu-Yong Jiao, Jiapeng Gao

Faculty of Engineering, China University of Geosciences, Wuhan, Hubei 430074, China



## ARTICLE INFO

## Keywords:

Mine earthquake  
Epicenter localization  
Fast Fourier Transform-Butterworth joint noise reduction method  
Rolling window ratio

## ABSTRACT

As the mining depth of coal resources increases, resulting in frequent mine earthquakes during mining. In this study, the rolling window ratio method is firstly chosen as the seismic phase recognition method to read the mine earthquake data received by the microseismic sensor. Secondly, the improved genetic algorithm is used as the optimization algorithm of the objective function to build the algorithmic framework of accurate inverse localization of mine earthquake. Finally, the accuracy of this algorithm for seismic source localization is validated using actual engineering cases. Results show that the first arrival time extraction by the rolling window ratio method has the advantages of high accuracy and fast algorithm operation speed. The Fast Fourier Transform-Butterworth joint noise reduction method has a good noise reduction effect, which successfully suppressing noise outside the mine earthquake signal and effectively improving the issue of excessive noise in the mine earthquake signal. Compared to microseismic monitoring data, the localization error for mine earthquakes remains within 5%.

## 1. Introduction

Coal is the dominant energy source in China, with coal consumption accounting for more than 50% of China's total energy consumption. The status of coal as the main source of energy cannot be changed for a considerable period of time. With the increase of mining depth of China's coal resources, strong mine earthquakes occur frequently, which seriously affects the efficient mining of coal resources [1,2]. Mine earthquake is a kind of response of coal and rock body to regional or local stress adjustment in the process of coal mining. It is usually accompanied by energy release and vibration, and is essentially caused by the presence of high stresses or high stress differentials in the coal rock mass [3,4]. Microseismic monitoring is a kind of geophysical technology for monitoring the effects of production activities by observing and analyzing the microseismic events in production activities [5]. Microseismic monitoring is now widely used in various fields such as geothermal development [6], slope stability study [7], hydraulic fracturing [8], and mining [9].

Many scholars have conducted a lot of research on seismic source localization methods. Waldhauser used a double-difference objective function to constrain the location estimation based on simulated arrival time differences and actual arrival time differences of two events [10].

This approach aims to reduce the impact of complex propagation media on the accuracy of location estimation and improve the algorithm's robustness against noise. More and more optimization algorithms have been applied to source location, such as Genetic Algorithm proposed by Holland [11], Particle Swarm Optimization Algorithm proposed by Kennedy [12], Grey Wolf Algorithm and Moth Flame Optimization Algorithm proposed successively by Mirjalili [13,14]. Li and other scholars proposed and analyzed the error space of microseismic source localization [15]. On this basis, a nonlinear microseismic source localization method based on the simplex method is proposed. Combining inverse fold product interferometry with interferometric cross-correlation bias, Wu *et al.* proposed inverse fold product bias and applied it to microseismic localization data for hydraulic fracturing [16]. Zhou used three meta-heuristic optimization algorithms to improve the performance of interlocking stacking methods for localization [17]. Wu proposed a new microseismic localization method, analyzed the factors affecting the source localization accuracy, combined the L2 paradigm HO variance function to improve the localization accuracy, and finally used a particle swarm optimization algorithm to search for the localization position [18].

In seismic source localization, the accuracy of seismic phase identification directly affects the accuracy of seismic source localization

\* Corresponding author.

E-mail address: [zoujunpeng@cug.edu.cn](mailto:zoujunpeng@cug.edu.cn) (J. Zou).<https://doi.org/10.1016/j.deepr.2024.100164>

Received 18 July 2024; Received in revised form 24 October 2024; Accepted 26 October 2024

Available online 2 November 2024

2949-9305/© 2025 The Author(s). Publishing services by Elsevier B.V. on behalf of KeAi Communications Co. Ltd This is an open access article under the CC BY-NC-ND license (<http://creativecommons.org/licenses/by-nc-nd/4.0/>).

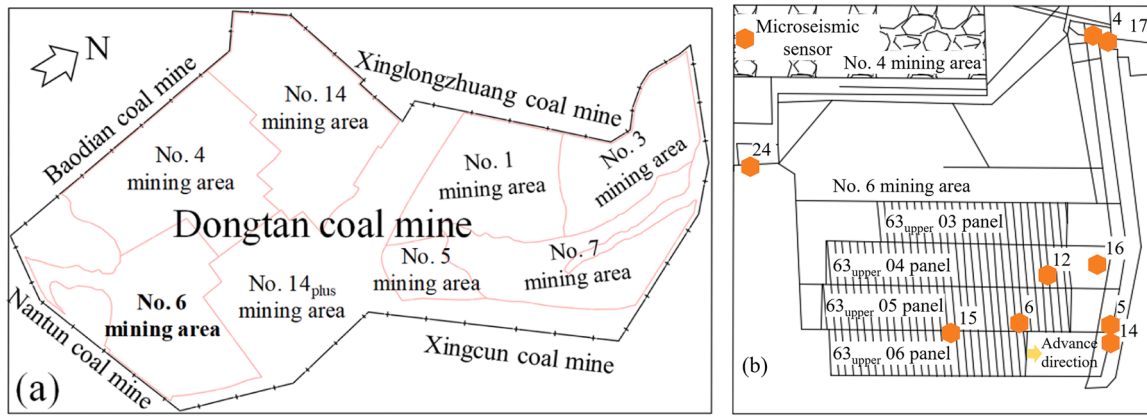


Fig. 1. Diagram of distribution of the mining areas of Dongtan coal mine and microseismic sensor arrangement in mining area.

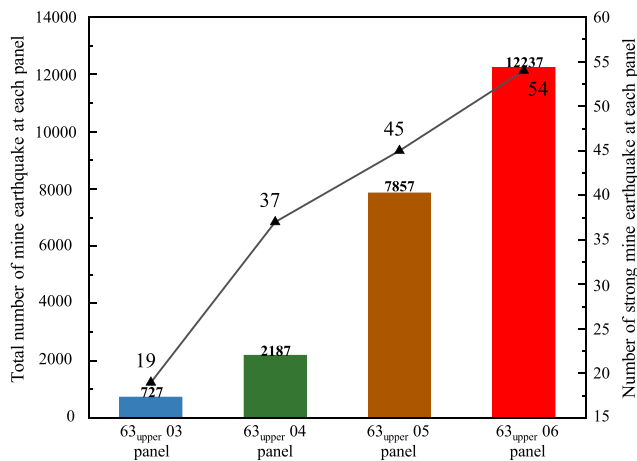


Fig. 2. Total number of occurrences of mine earthquakes and number of occurrences of strong mine earthquakes in each panel of the No.6 mining areas.

Table 1  
Six large-energy mine earthquakes.

Date	Time	X (m)	Y (m)	Z (m)	Energy (J)
2020/3/23	5:28:00	39489286.50	3921544.00	-454.03	$2.39 \times 10^6$
2020/4/15	8:33:04	39489265.57	3921197.41	-557.71	$2.70 \times 10^6$
2020/4/17	8:21:51	39489172.37	3921438.26	-483.05	$2.20 \times 10^6$
2020/5/15	17:55:33	39489185.23	3921472.92	-447.26	$6.81 \times 10^6$
2020/6/10	19:18:59	39489332.59	3921128.00	-518.00	$2.29 \times 10^6$
2020/11/30	9:41:49	39489759.29	3920929.36	-508.50	$2.38 \times 10^6$

interpretation. Many researchers and scholars have studied and explored the seismic phase identification techniques of seismic signals and proposed many automatic phase identification algorithms. Chen proposed a pickup method based on a fuzzy clustering algorithm for seeded seismic phase walk time [19]. Perol *et al.* first applied convolutional neural networks to seismic event detection as well as source location determination [20]. Ross applied the convolutional neural network in deep learning to seismic P-wave first-arrival time extraction, abandoning the process of feature extraction and instead using the seismic record as input directly with only a small amount of pre-processing [21]. Zhang *et al.* utilized the feature extraction capability of deep learning to propose a multi-channel joint earthquake phase identification and first-to-pickup method based on U-net [22]. Wu *et al.* has proposed a high-resolution hybrid imaging condition (HIC) method for microseismic source location, who find that cross-correlation migration

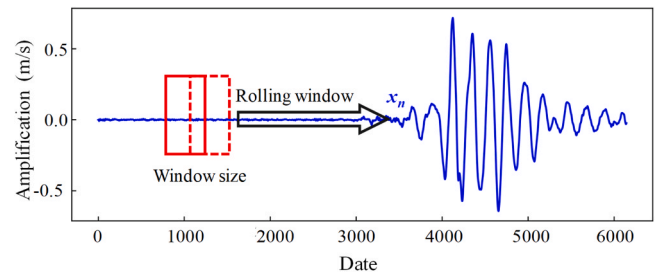


Fig. 3. Schematic of the sliding window of the rolling window ratio.

(CCM)-HIC could noticeably improve the spatial resolution and stability of source location images, reaching a better compromise between summation imaging condition (SIC) and multiplication imaging condition (MIC), particularly in the presence of strong noise [23]. Wu and Wang proposed a deblurring filter (DLSIM) to obtain high-resolution microseismic source locations at a low computational cost. DLSIM approximates the inverse Hessian with an inexpensive deblurring (nonstationary) filter to eliminate the blurring effect of the Hessian matrix. It could significantly accelerate the convergence rate of the least-squares inversion and, meanwhile, reduce the computational cost owing to its fewer number of iterations [24]. However, the existing microseismic monitoring technology in coal mines still has limitations in terms of signal separation, signal transmission, and positioning accuracy.

In previous studies, various algorithms have been widely applied to mine earthquake source localisation, but less research has been conducted on microseismic phase extraction and identification. In this study, the rolling window ratio method is firstly chosen as the seismic phase recognition method to read the mine earthquake data received by the microseismic sensor. Secondly, the improved genetic algorithm is used as the optimization algorithm of the objective function to build the algorithmic framework of accurate inverse localization of mine earthquake. Finally, the accuracy of the algorithm for seismic source localization is verified using actual engineering cases.

Table 2  
Sliding window extraction results for different window sizes.

Date	Window_len	Pick up time (s)	Calculating runtime (s)
2020/1/2	1	0.408	2.01586
	2	0.322	2.01071
	4	0.406	2.01011
2020/9/25	1	0.844	2.01529
	2	0.840	2.00158
	4	0.856	2.01293

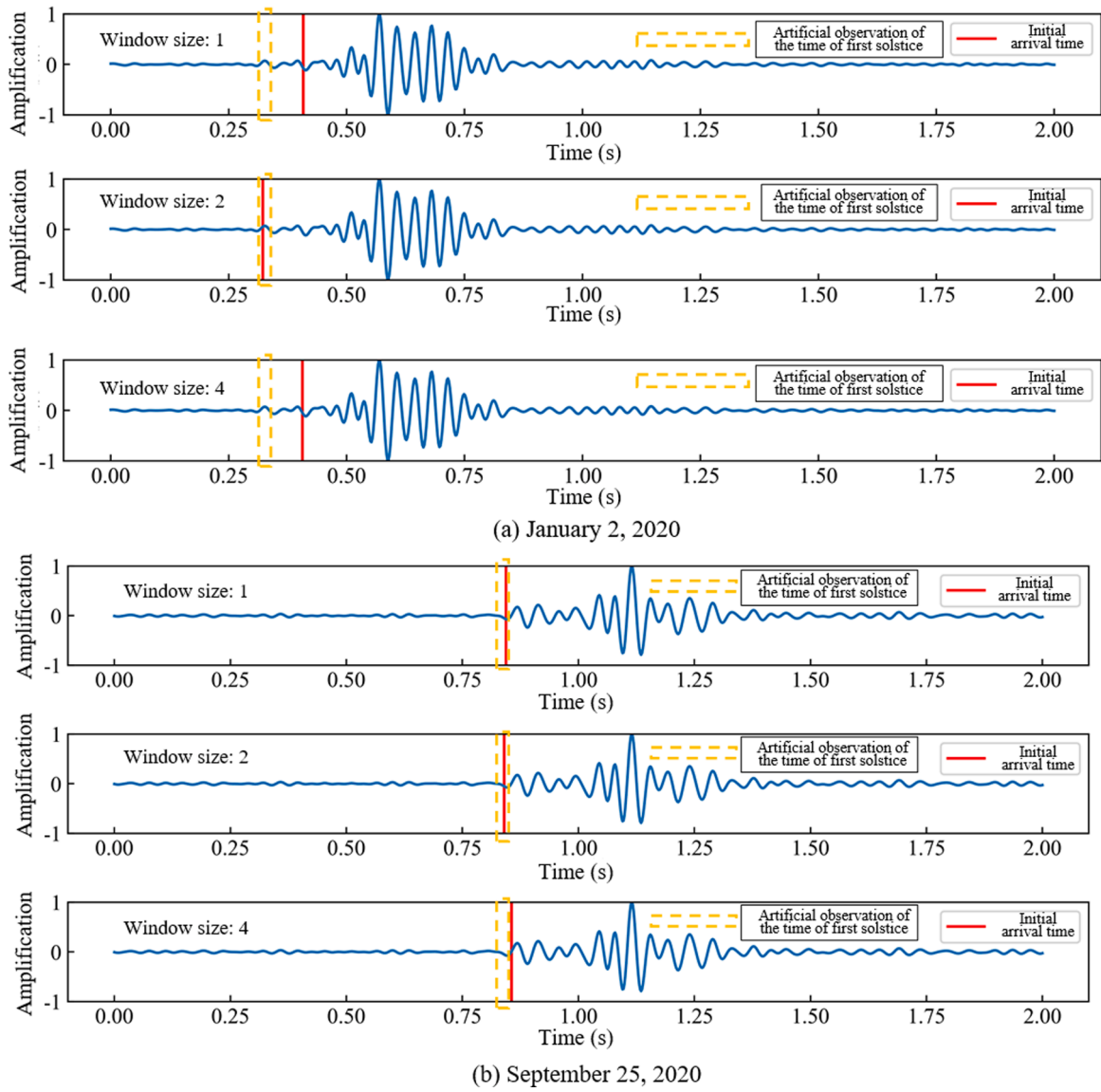


Fig. 4. Results of different window extraction by sliding time window energy ratio method.

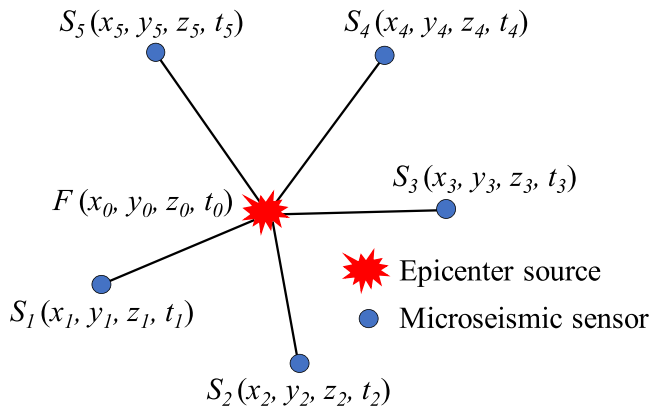


Fig. 5. Schematic diagram of mine earthquake localization.

## 2. Engineering background

Dongtan coal mine is located in Zoucheng City, Shandong Province, China. The No.6 mining area is located on the southern flank of the

Dongtan coal mine. The mining area is about 3.4 km long from east to west and 1.8–2.8 km wide from north to south. The surface elevation of the No.6 mining areas is from +43.52 m to +55.51 m, with an average of +48.43 m. The 63<sub>upper06</sub> panel is designed with a length of 1500 m. As of October 2023, the 63<sub>upper06</sub> panel has been mined back for 1070 m. The geographic location of Dongtan coal mine and the distribution of the mining areas, and the microseismic sensors are arranged as shown in Fig. 1.

As of November 30, 2023, a total of 12237 mine earthquakes have been monitored around the 63<sub>upper06</sub> panel, among which the number of mine earthquakes with energy greater than  $1 \times 10^5$  J (strong mine earthquake) is 54, accounting for 0.44 % of the total, the number of mine earthquakes with energy greater than  $1 \times 10^4$  J is 715, accounting for 5.85 % of the total (Fig. 2). The number of mine earthquakes with a magnitude of 1 or higher (energy greater than  $2 \times 10^6$  J) is 6 times. The locations and occurrence times of these six large mine earthquakes are shown in Table 1.

## 3. Mine earthquake localization inversion algorithm

Locating the source of a mine earthquake first requires the identification of a mine earthquake event. The main seismic phase

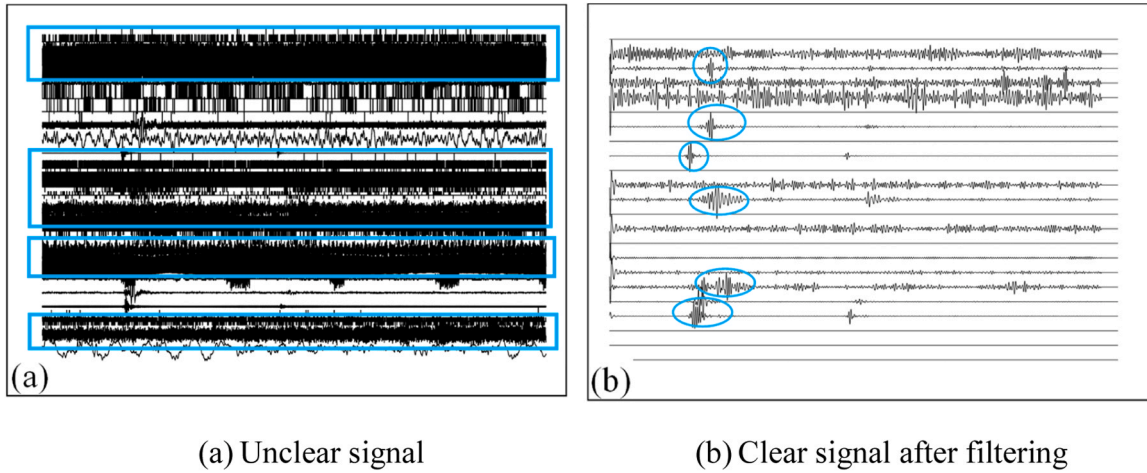


Fig. 6. Mine earthquake wave data reading and filtering.

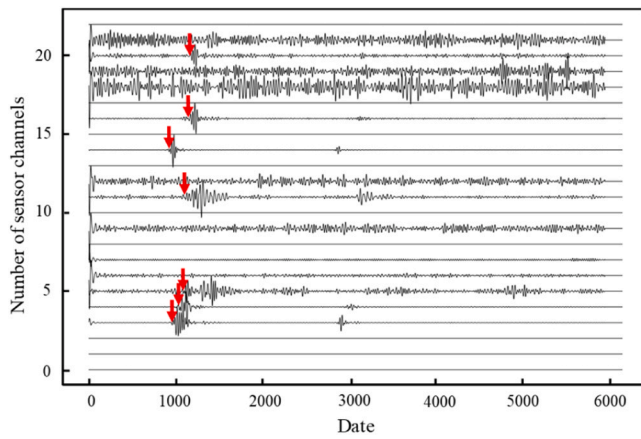


Fig. 7. Automatic extraction of P-wave first arrival time.

identification method used in this study is the rolling window ratio method, which is widely used in the field of microseismic initial to automatic pick up. For a rolling window of the same length, the difference between the energy in the rolling window after the moment of arrival of the mine earthquake signal and the energy in the rolling window before its arrival is relatively large. By detecting the sudden change in the value of the ratio between the two, a mine earthquake event can be identified and its wave arrival time can be determined. The specific steps are as follows:

- 1) First assume that the mine earthquake recording channel is  $[X_n]$ .
- 2) Design a sliding window  $M$  with a settable width for calculating the sum of the mine earthquake data within the window, as shown in Fig. 3.

The energy ratio between the rear rolling window and the front rolling window could be expressed as shown in Eq. (1). A stabilization factor  $\sigma$  is usually introduced to enhance its stability, and its value is generally much smaller than the energy value of the front rolling window, which is usually taken as the average energy value of the channel background noise, as shown in Eq. (2).

$$R_i = \left[ \frac{\sum_{k=i}^{i+M-1} x_k^2}{\sum_{k=i-M}^{i-1} x_k^2} \right]^{1/2} \dots \quad (1)$$

$$R_i = \left[ \frac{\sum_{k=i}^{i+M-1} x_k^2 + \sigma}{\sum_{k=i-M}^{i-1} x_k^2 + \sigma} \right]^{1/2} \dots \quad (2)$$

When the first arrival wave arrives, the energy ratio  $R_i$  between the rear rolling window and the front rolling window at the sampling point of the wave arrival moment is theoretically maximized without taking into account the influence of noise and other factors. Pick up the time corresponding to the maximum value of  $R_i$  that is the first arrival moment of the mine earthquake wave, at this time  $i$  is the number of sample points of the first arrival time of the P-wave, the first arrival time that is the ratio of the number of sample points to the sampling frequency (sample rate) is named the first arrival time (Eq. (3)).

$$t = \frac{i}{f_{\text{sample-rate}}} \dots \quad (3)$$

The rolling window was proposed to overcome the shortcomings of the fixed rolling window, and its main working principle is that the rolling window is not fixed, but starts from the beginning of the signal and moves towards the ending of the signal.  $M$  is the sampling interval for each move is set on a case-by-case basis in the calculation, and is usually set to 1. The ratio of the energy size of the front and back rolling windows is calculated every time the rolling window moves, and then the first mutation value is found from these energy ratios, and the threshold value of this mutation value is then used to find the sampling point with the largest amplitude in the corresponding rolling window corresponding to the time that is the time of the first arrival, as shown in Fig. 3.

The sliding window program was written using the Python 64-bit version of the program configured in the Anaconda 3 environment, and the compiler chosen was the Spyder compiler that comes with Anaconda 3. The computing processor was an Intel(R) Core(TM) i5-10500 CPU @ 3.10 GHz.

The program set the sliding window size window\_len and mutation threshold of the two parameters, window\_len selected 1, 2, 4 window, while using Python comes with the program running time calculation toolkit, calculate the time that the program is running in order to carry out the calculation of speed. Since the data were normalized, the data range were all in the range of (-1,1), and after many trials it was found that it was more reasonable to choose 1.01 for the mutation threshold. Comparison of the impact of the difference in the size of the window on the results, selected events occurring at the moment of January 2, 2020 16:55:15, sensor number 15 of the mine earthquake data, events occurring at the moment of September 25, 2020 10:19:50, the sensor number 15 of the mine earthquake data. The results of the calculations and the calculation of the running time are shown in Table 2, Fig. 4.

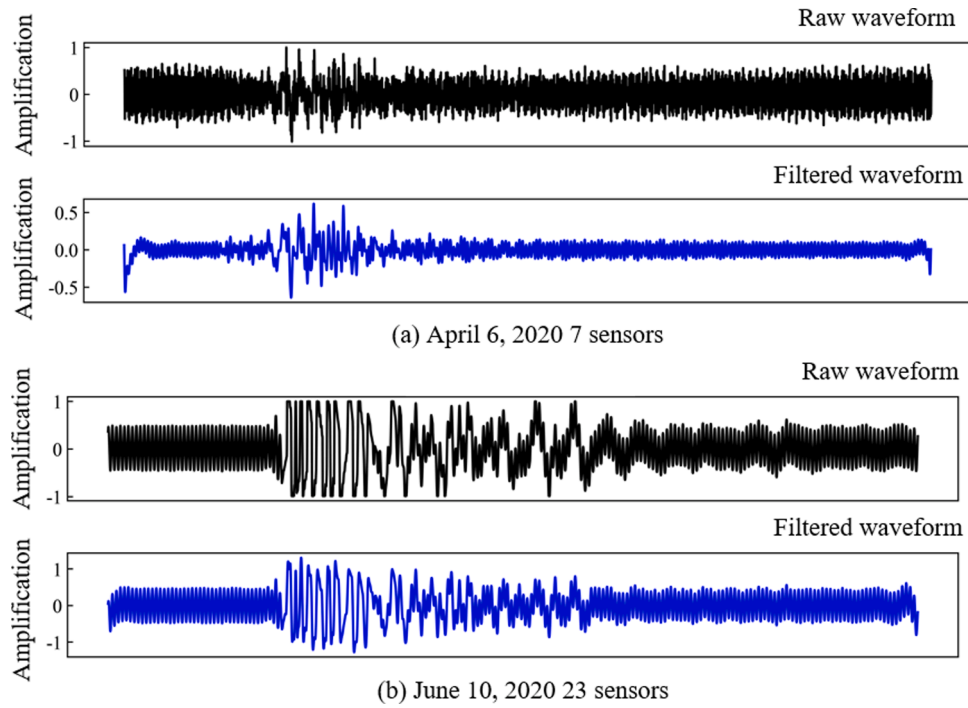


Fig. 8. FFT-Butterworth joint filtering noise reduction effect.

Table 3

Large-energy mine earthquakes in 63<sub>upper</sub> 06 panel.

Date	Time	X (m)	Y (m)	Z (m)	Energy (10 <sup>5</sup> J)
2020/3/23	5:28:00	39489286.50	3921544.55	-454.03	23.90
2020/4/6	23:23:53	39489224.52	3921426.82	-461.20	6.23
2020/5/15	17:55:33	39489185.23	3921472.92	-447.26	68.10
2020/6/10	19:18:59	39489332.59	3921128.00	-518.00	22.90
2020/7/12	16:29:30	39489334.96	3921317.72	-509.09	8.38

Microseismic monitoring provides sufficient basis for the stability evaluation of coal rock bodies by obtaining the signals emitted from the rupture of coal rock bodies [18]. First, a number of waveform sensors are placed in mining area to form a monitoring zone. If a mine earthquake occurs, the sensors capture the signal and convert it into an electrical signal. Multiple sensors acquire data are used to determine position and velocity in the localization equations to localize the mine earthquake source (Fig. 5). The basic equation of localization used in this study is the arrival time difference method, described by a set of nonlinear equations (Eq. (4)):

$$\sqrt{(x_0 - x_i)^2 + (y_0 - y_i)^2 + (z_0 - z_i)^2} = v_0(t_i - t_0) \dots \quad (4)$$

Table 4

Inversion results for large-energy mine earthquakes.

Date	Time	Actual mine earthquake source location			Calculated mine earthquake source location		
		X (m)	Y (m)	Z (m)	X (m)	Y (m)	Z (m)
2020/3/23	5:28:00	(39489)286.50	(3921)544.55	-454.03	(39489)312.46	(3921)525.62	-465.43
2020/4/6	23:23:53	(39489)224.52	(3921)426.82	-471.20	(39489)241.15	(3921)441.77	-481.47
2020/5/15	17:55:33	(39489)185.23	(3921)472.92	-447.26	(39489)174.09	(3921)496.21	-441.92
2020/6/10	19:18:59	(39489)332.59	(3921)128.00	-518.00	(39489)352.59	(3921)141.00	-539.11
2020/7/12	16:29:30	(39489)334.96	(3921)317.72	-509.09	(39489)345.96	(3921)346.72	-533.14

where

- $x, y, z$  are the three-dimensional positions in space;
- $x_0, y_0, z_0$  are the locations of the mine earthquake source;
- $x_i, y_i, z_i$  are the locations of the  $i$ th sensor;
- $t_0$  is the start time of the occurrence of the mine earthquake;
- $t_i$  is the time to the sensor;
- $v$  is the propagation velocity of the P-wave;
- $i = 1, 2, 3, 4 \dots n$  ( $n$  denotes the number of sensors).

Due to complex mathematical models that cannot be solved directly, we need to use optimization algorithms to solve the objective function. Genetic algorithms have been widely used for their ability to search globally for the optimal solution of an objective function. Currently, the development of optimization algorithms is rapid, among which genetic algorithm, particle swarm optimization algorithm, simulated annealing algorithm are widely used in mine earthquake monitoring. Reeves mentioned several advantages of genetic algorithm compared with the other two algorithms in his study: 1) Strong global search ability: genetic algorithm has strong global search ability through crossover, mutation and selection operations, and can find the global optimal solution in the complex search space. In contrast, particle swarm algorithm and simulated annealing algorithm may not perform as well as genetic algorithm in global search; 2) Relatively easy to adjust parameters: Genetic algorithm is relatively easy to adjust parameters compared with particle swarm algorithm and simulated annealing algorithm. For example, the adjustment of parameters such as crossover rate and mutation rate can directly affect the performance of the algorithm, and the adjustment of these parameters is relatively intuitive in genetic algorithm [25]. The

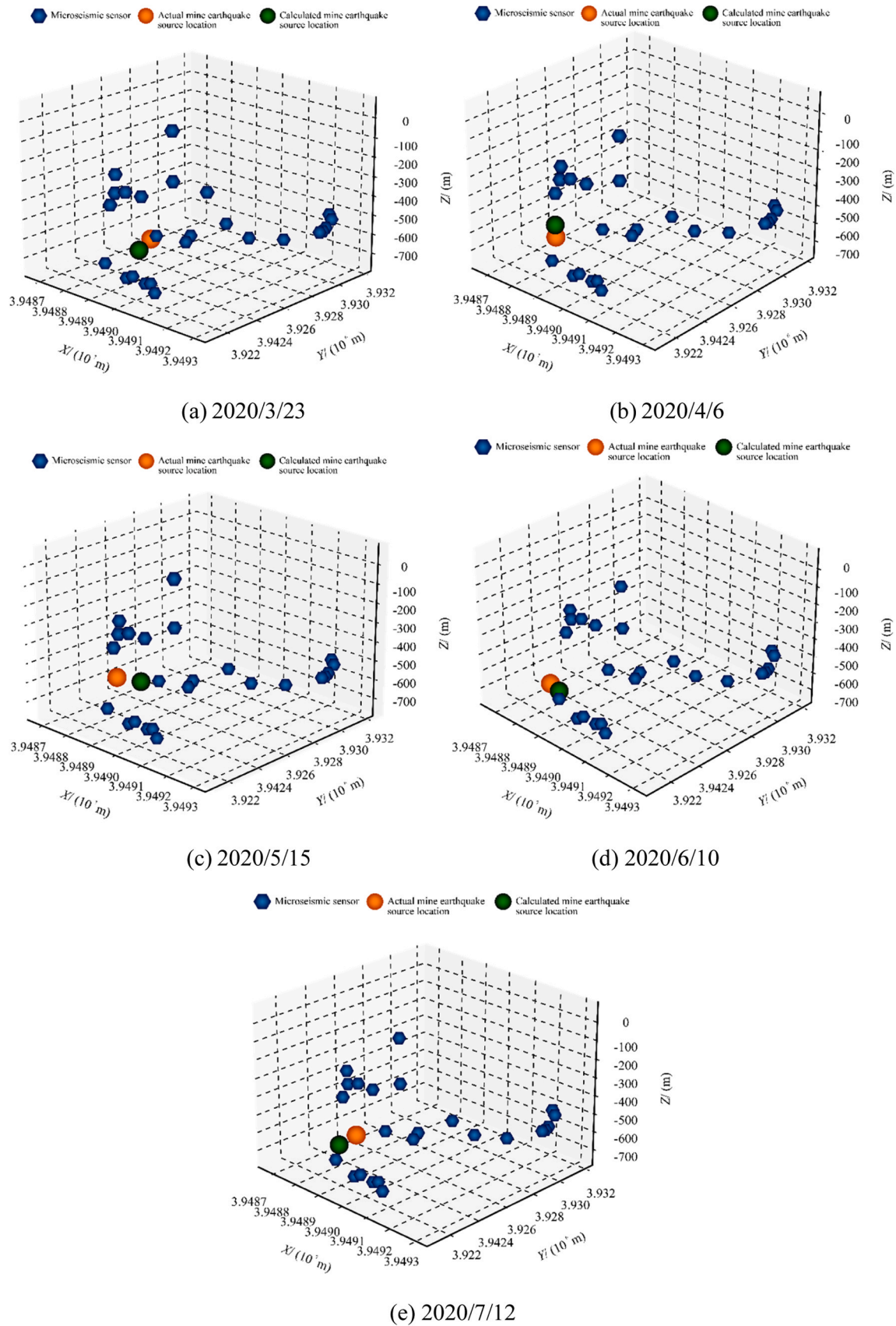


Fig. 9. A part of large-energy mine earthquakes localization inversion results.

**Table 5**  
Comparison of mine earthquake source location results error analysis results.

Date	Time	Inaccuracy (%)
2020/3/23	5:28:00	4.4
2020/4/6	23:23:53	2.7
2020/5/15	17:55:33	4.8
2020/6/10	19:18:59	5.0
2020/7/12	16:29:30	5.5

improved genetic algorithm is optimized and improved compared with the traditional genetic algorithm in terms of algorithm structure, operation mode, parameter settings, and application scenarios. These improvements make the improved genetic algorithm have higher efficiency and better performance when dealing with complex optimization problems.

The optimization method selected in this study uses genetic algorithm, combined with Fast Fourier Transform (FFT)-Butterworth filter joint noise reduction method and rolling window ratio method to localize the large-energy mine earthquakes. The optimization process requires further simplification of the objective function. The time  $t_i'$  for the propagation of the mine earthquake wave through the coal rock body to the event signal received by each sensor, as shown in Eq. (5). In field engineering, the medium of the observation area is not homogeneous, and there are errors in the arrival time recorded by the sensors, so there are residuals in the travel time of mine earthquake waves. Let the ration of the sum of the travel time residuals of each sensor to the number of sensors be the average travel time residual  $\delta$ , as shown in Eq. (6). A certain threshold and maximum number of iterations are set, and the mine earthquake source parameters can be output when  $\delta$  is smaller than this threshold or the maximum number of iterations is reached. During the iteration process, if  $\delta$  does not reach a certain threshold, the last  $\delta$  is compared with the  $\delta'$  obtained from this calculation, and the mine earthquake parameters are then subjected to mutation and inheritance in the genetic algorithm on the basis of the one with a smaller  $\delta$ .

$$t_i = \frac{\sqrt{(x_0 - x_i)^2 + (y_0 - y_i)^2 + (z_0 - z_i)^2}}{v_0} + t_0 \dots \quad (5)$$

$$\delta = \frac{\sum_{i=1}^n (t_i - t_i')}{n} \dots \quad (6)$$

#### 4. Application and validation of mine earthquake localization algorithms

In order to achieve an accurate inversion of the mine earthquake source location, it is necessary to be able to acquire the mine earthquake waves. After first reading the mine earthquake wave data, a bandpass filter is used to extract the information in the initial specific frequency range while removing the noise. The bandpass filter has two cutoff frequencies, a low-frequency cutoff ( $f_{low}$ ) and a high-frequency cutoff ( $f_{high}$ ) frequency, which define the range of frequencies allowed to pass through and are called the Passband. The passband contains the frequency components between the low-frequency cutoff frequency and the high-frequency cutoff frequency. The channel signals that have absolutely no way to participate in the calculation are then removed, making the mine earthquake noise clearer the rolling window ratio method more accurate in extracting the first arrival time of the P-wave, as shown in Fig. 6 and Fig. 7.

Butterworth bandpass filter processing is the process of noise reduction of the clearer signals to retain only the information of the frequencies near the mine earthquake signals. In this study, clear signals, clearer signals, and poorly defined signals with severe interference were selected for comparison of the noise reduction process. The April 6, 2020

event 7 sensor, and the June 10, 2020 event 23 sensor were selected. The upper and lower filter limits were selected as 1 Hz and 30 Hz, respectively, and signals outside this frequency range were suppressed. The signal butter function in the Scipy toolkit in Python is used in this study, as the mine earthquake signal contains many aspects of noise directly choose the filtering effect is best sixth order Butterworth bandpass filter with a sampling frequency of 500 Hz. Both the original and filtered waveforms are shown in Fig. 8. As seen in Fig. 8(a) and (b), the joint FFT-Butterworth method works significantly on the clearer signals and successfully suppresses the noise outside the signal, resulting in a smooth waveform curve.

The initial values of  $x_0, y_0, z_0$  are assumed to be the center of the mine range, the initial value of  $v$  is assumed to be 4000 km/s, and the initial value of  $t_0$  is set to be the moment of 0 s, and the actual propagation time of the P-wave from the mine earthquake source to the microseismic sensors is the arrival moment recorded by the sensors. The sampling frequency of the microseismic sensor  $f_{sample-rate}=500$  Hz; set the rolling window ratio window  $2M=10$ ; set the minimum average travel time residual  $\delta_{min}=0.001$  s (output the mine earthquake source parameter when  $\delta < \delta_{min}$ ); and set the maximum number of cycles  $num=50000$  (output the mine earthquake source parameter when the number of genetic variations is greater than 50000 times). Based on several localization tests, the initial parameters of the mine earthquake source have been tuned to be more reasonable.

The calculated mine earthquake source location results were compared and analyzed with the actual mine earthquake source location results, and the error analysis was performed using Eq. (7) [18]:

$$Q = \frac{\sqrt{x_1^2 - x_2^2 + y_1^2 - y_2^2 + z_1^2 - z_2^2}}{\sqrt{x_1^2 + y_1^2 + z_1^2}} \dots \quad (7)$$

Where

$x_1, y_1, z_1$  is the coordinate parameter calculated by the SOS microseismic system;

$x_2, y_2, z_2$  is the coordinate parameter calculated by the method of this study, the physical meaning of which is to use the distance error to the origin to portray the localization error.

Five typical large-energy mine earthquakes that occurred in the 63<sub>upper</sub> 06 panel are shown in Table 3. The inversion results of the mine earthquakes are shown in Table 4 and Fig. 9, and the error results are shown in Table 5.

Compared to the mine earthquake data from microseismic monitoring, the mine earthquake localization algorithm in localizing the five large-energy mine earthquakes, with localization errors within 5%. The reason for the large errors in some of the data may be related to the iteration accuracy of the optimisation algorithm.

#### 5. Conclusions

- 1) The rolling window ratio method for first arrival time extraction has the advantages of high accuracy and fast algorithmic computation.
- 2) The Fast Fourier Transform-Butterworth joint noise reduction method has a good noise reduction effect, which successfully suppressing noise outside the mine earthquake signal and effectively improving the issue of excessive noise in the mine earthquake signal.
- 3) Compared to the mine earthquakes from microseismic monitoring, the localization errors for large-energy mine earthquakes are within 5%.

#### CRedit authorship contribution statement

**Quan Zhang:** Writing – review & editing, Writing – original draft, Formal analysis. **Junpeng Zou:** Writing – review & editing, Resources, Funding acquisition. **Yu-Yong Jiao:** Resources, Funding acquisition. **Jiapeng Gao:** Investigation, Data curation.

## Declaration of Competing Interest

The authors declare that they have no known competing financial interests or personal relationships that could have appeared to influence the work reported in this paper.

## Acknowledgments

This work is supported by the Shandong Energy Group (No. SNKJ2022A01-R26).

## References

- [1] S.J. Gibowicz, A. Kijko, *An introduction to mining seismology*, Elsevier, 2013.
- [2] T.I. Urbancic, C.I. Trifu, Recent advances in seismic monitoring technology at Canadian mines, *J. Appl. Geophys.* 45 (4) (2000) 225–237.
- [3] L.M. Dou, J.R. Cao, A.Y. Cao, Y.J. Chai, J.Z. Bai, J.L. Kan, Research on types of coal mine tremor and propagation law of shock Waves, *Coal Sci. Technol.* 49 (6) (2021) 23–31.
- [4] J.B. Zhu, B.W. Ma, H.P. Xie, F. Gao, H.W. Zhou, C.T. Zhou, F.R. Zheng, Differences and connections between mining seismicity and coal bursts in coal mines and preliminary study on coal bursts induced by mining seismicity, *J. China Coal Soc.* 47 (09) (2022) 3396–3409.
- [5] B.X. Zhao, Z.R. Wang, R. Liu, L.Q. Lei, Review of Microseismic monitoring technology research, *Prog. Geophys.* 29 (4) (2014) 1882–1888.
- [6] R.V. Ry, D.P. Sahara, M. Rohaman, Implementation of GMSTech—a New Practical Software for Microseismic Data Processing—for Estimating Event Source Parameters//*Journal of Physics: Conference Series*, 1204, IOP Publishing, 2019 012096.
- [7] N.W. Xu, F. Dai, Z.Z. Liang, Z. Zhou, C. Sha, C.A. Tang, The dynamic evaluation of rock slope stability considering the effects of microseismic damage, *Rock. Mech. Rock. Eng.* 47 (2014) 621–642.
- [8] Y. Lin, H. Zhang, Imaging hydraulic fractures by microseismic migration for downhole monitoring system, *Phys. Earth Planet. Inter.* 261 (2016) 88–97.
- [9] A.Y. Cao, L.M. Dou, C.B. Wang, X.X. Yao, J.Y. Dong, Y. Gu, Microseismic precursory characteristics of rock burst hazard in mining areas near a large residual coal pillar: a case study from Xuzhuang coal mine, Xuzhou, China, *Rock. Mech. Rock. Eng.* 49 (2016) 4407–4422.
- [10] D. Gajewski, E. Tessmer, Revere modeling for seismic events characterization, *Geophys. J. Int.* 163 (2005) 276–284.
- [11] J.H. Holland, Genetic algorithms, *Sci. Am.* 267 (1) (1992) 66–73.
- [12] J. Kennedy, R. Eberhart, Particle swarm optimization, *Proc. ICNN'95-Int. Conf. Neural Netw.* 4 (1995) 1942–1948.
- [13] S. Mirjalili, Moth-flame optimization algorithm: A novel nature-inspired heuristic paradigm, *Knowl.-Based Syst.* 89 (2015) 228–249.
- [14] S. Mirjalili, S.M. Mirjalili, A. Lewis, Grey wolf optimizer, *Adv. Eng. Softw.* 69 (2014) 46–61.
- [15] N. Li, E. Wang, M. Ge, Z.Y. Sun, A nonlinear microseismic source location method based on Simplex method and its residual analysis, *Arab. J. Geosci.* 7 (2014) 4477–4486.
- [16] S. Wu, Y. Wang, Y. Zheng, X. Chang, Microseismic source locations with deconvolution migration, *Geophys. J. Int.* 212 (3) (2018) 2088–2115.
- [17] J. Zhou, X.J. Shen, Y.G. Qiu, X.Z. Shi, M. Khandelwal, Cross-correlation stacking-based microseismic source location using three metaheuristic optimization algorithms, *Tunn. Undergr. Space Technol.* 126 (2022) 104570.
- [18] L.Z. Wu, S.H. Li, R.Q. Huang, S.Y. Wang, Micro-seismic source location determined by a modified objective function, *Eng. Comput.* 36 (2020) 1849–1856.
- [19] Y.K. Chen, Automatic microseismic event picking via unsupervised machine learning, *Geophys. J. Int.* 222 (3) (2020) 1750–1764.
- [20] T. Perol, M. Gharbi, M. Denolle, Convolutional neural network for earthquake detection and location, *Sci. Adv.* 4 (2) (2018) e1700578.
- [21] Z.E. Ross, M.A. Meier, E. Hauksson, P wave arrival picking and first-motion polarity determination with deep learning, *J. Geophys. Res.: Solid Earth* 123 (6) (2018) 5120–5129.
- [22] Y.L. Zhang, Z.C. Yu, T.Y. Hu, C. Chuan, Multi-trace joint downhole microseismic phase detection and arrival picking method based on U-Net, *Chin. J. Geophys.* 64 (6) (2021) 2073–2085.
- [23] S.J. Wu, Y.B. Wang, F. Xie, X. Chang, Crosscorrelation migration of microseismic source locations with hybrid imaging condition, *Geophysics* 87 (1) (2022) KS17–KS31.
- [24] S.J. Wu, Y.B. Wang, Least-squares interferometric migration of microseismic source location with a deblurring filter, *Geophysic* 88 (2) (2023) L37–L52.
- [25] C.R. Reeves, Genetic algorithms, *Handb. metaheuristics* (2010) 109–139.



**Zou Junpeng**, Professor and Doctoral Supervisor at China University of Geosciences. His main research interests focus on the disaster mechanism and prevention technology of tunnel and deep earth engineering. He has led nine projects, such as National Natural Science Foundation projects. His scientific research has been awarded 1 Second Prize of National Science and Technology Progress Award.